

FIGURE S1

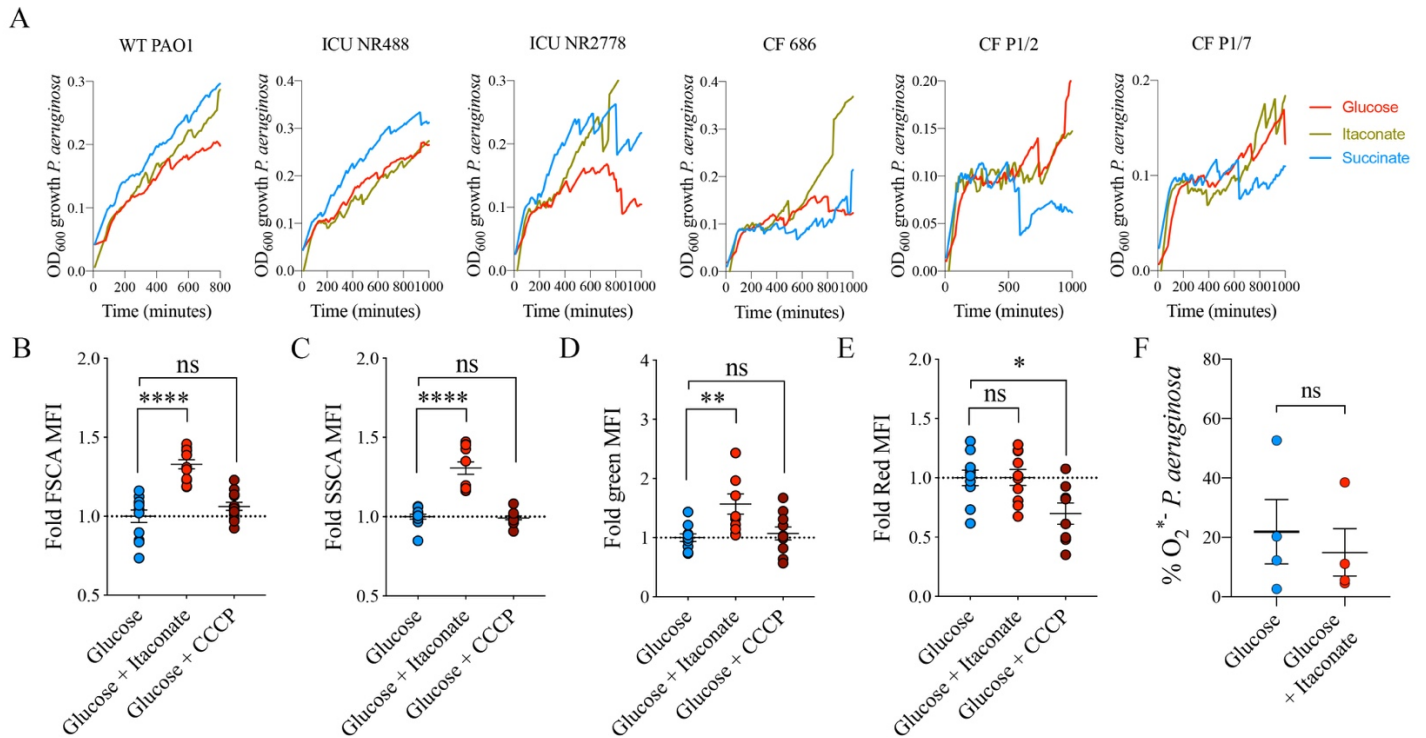


FIGURE S1, related to FIGURE 1. Itaconate metabolism is associated with *in vivo* host adaptation and membrane deregulations in *P. aeruginosa*.

A) *P. aeruginosa* growth curves in M9 media supplemented either with itaconate, succinate or glucose for PAO1, two ICU isolates (NR488, NR2778) and 3 CF clinical isolates (CF 686, CF P 1/2, CF P1/7).

B-F) Bacterial size (Forward FSCA) (B), bacterial surface granularity (Scatter SSCA) (C), DiOC₂(3) green emission (D) and DiOC₂(3) red emission (E) in *P. aeruginosa* PAO1 incubated overnight in either glucose or glucose + itaconate. CCCP, membrane potential uncoupler, was used as a positive control to determine DiOC₂(3) specificity.

F) Anion superoxide (O₂⁻) production by flow cytometry using Mitosox in *P. aeruginosa* PAO1 incubated either in glucose or glucose + itaconate.

A are representative curves from n=2. **B-F**, from n=3. In **B-F**, data are shown as average +/- SEM. **B-E**: One-Way ANOVA; **F**: t-Student. ****: $P < 0.0001$; **: $P < 0.01$; *: $P < 0.05$; ns: non-significant.

FIGURE S2

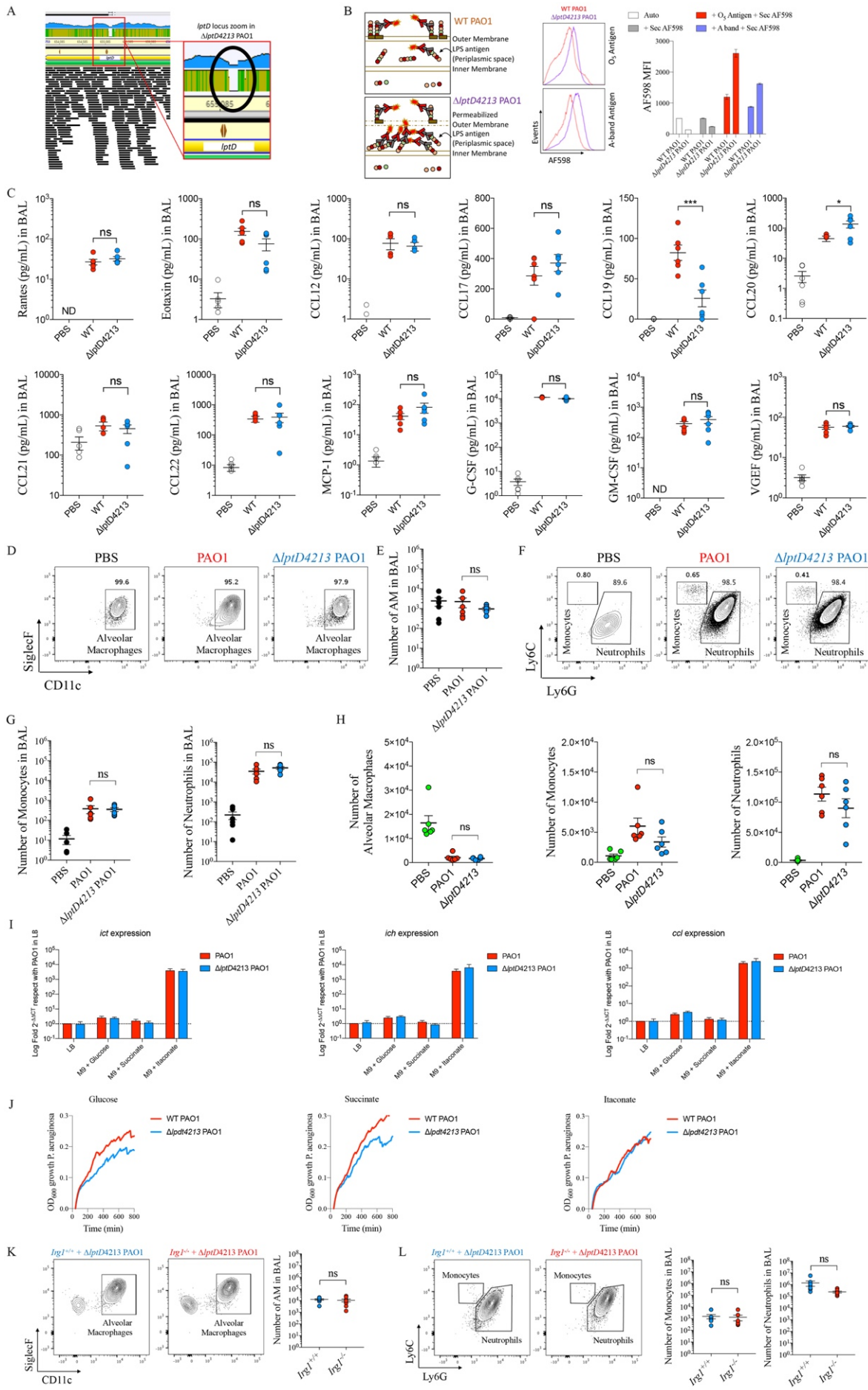


FIGURE S2, related to FIGURE 2. *lptD* deregulation conserves itaconate metabolism by PAO1.

A) In respect to WT PAO1, $\Delta lptD4213$ PAO1 exhibits a 69 nucleotide deletion (black circle) in the *lptD* gene that produces a truncated LptD protein lacking 23 amino acids.

B) Dysfunctional LptD produces membrane permeability and accumulation of LPS-associated sugars in the periplasmic space of *P. aeruginosa*. Anti-LPS antibodies penetrate the outer membrane and detect accumulated endotoxin-associated carbohydrates (middle histograms and right graphs, by flow cytometry). Anti-LPS carbohydrates antibodies used were anti O₅ antigen and anti A-band sugars.

C-H) BAL chemokines by ELISA (C) and myeloid cell numbers in BAL (D-G) and lungs (H) by flow cytometry from WT mice treated with PBS or infected for 16h either with WT PAO1 or $\Delta lptD4213$ PAO1.

I) Expression of *ict*, *ich* and *ccl* by qRT-PCR in WT PAO1 and $\Delta lptD4213$ PAO1 grown in different media.

J) Growth curves for WT PAO1 and $\Delta lptD4213$ PAO1 in M9 media supplemented either with succinate, glucose or itaconate.

K-L) Alveolar macrophages (K) and monocytes/neutrophils (L) by flow cytometry in *Irg1*^{+/+} and *Irg1*^{-/-} BAL from mice 16h-infected with $\Delta lptD4213$ PAO1.

Data are shown as average +/- SEM. **C-H** and **K-L** are from n=2 with a total of 6 mice. **C-H**: One-Way ANOVA; **K-L**: t-Student test. ***: $P < 0.001$; *: $P < 0.05$; ns: non-significant.

Figure S3

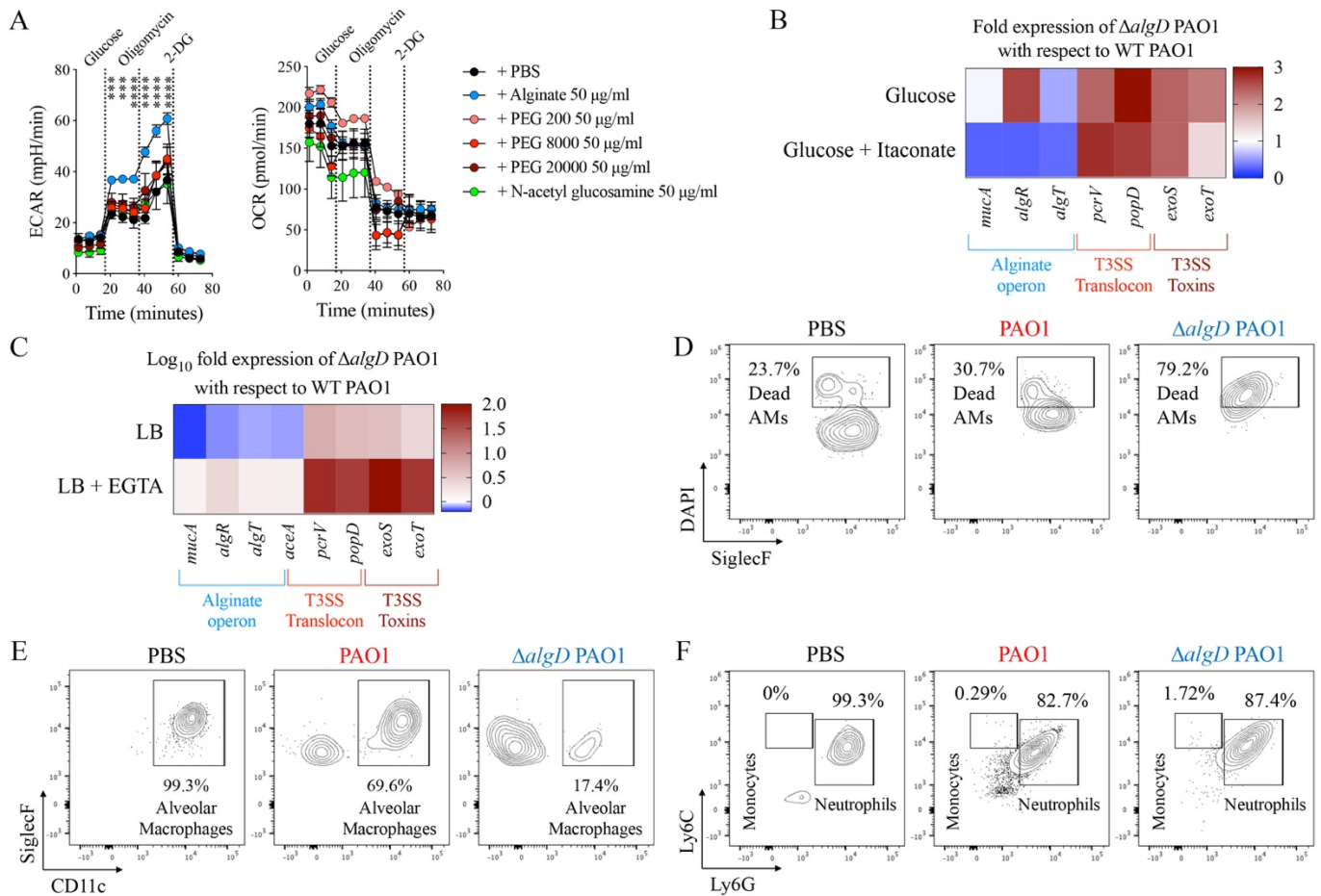


FIGURE S3, related to FIGURE 3, 4. Increased alginate production promotes myeloid cell activation and accumulation in the murine airway.

A) Glycolysis (ECAR) and oxygen consumption rates (OCR) by Seahorse technology of mouse BMDMs stimulated either with PBS, alginate, polyethylene glycol (200, 8000, 20000 MW) or N-acetyl glucosamine.

B) Respect with WT PAO1, fold expression of *mucA*, *algT*, *algR*, *pcrV*, *popD*, *exoS* and *exoT* by qRT-PCR for $\Delta algD$ PAO1 incubated in M9 + glucose or M9 + glucose + itaconate.

C) Respect with WT PAO1, Log₁₀ fold expression of *mucA*, *algT*, *algR*, *pcrV*, *popD*, *exoS* and *exoT* by qRT-PCR for $\Delta algD$ PAO1 incubated in LB treated or not with EGTA, which activates type 3 secretion system function.

D) DAPI⁺ staining (dead cells) for BAL alveolar macrophages from mice treated with PBS or infected either with WT and $\Delta algD$ PAO1.

E-F) Representative density plots for alveolar macrophages (E) and Ly6C^{high}Ly6G^{low/-} monocytes and Ly6C^{low/neg}Ly6G⁺ neutrophils (F) from BAL of WT mice treated with PBS or infected with PAO1 WT or $\Delta algD$ PAO1. Data are shown as average +/- SEM. A is from n=2. **A:** Two-Way ANOVA. **D-F:** In vivo data are from n=2 (7-8 mice total). ****: $P < 0.0001$; ***: $P < 0.001$; **: $P < 0.01$; ns: non-significant.

FIGURE S4

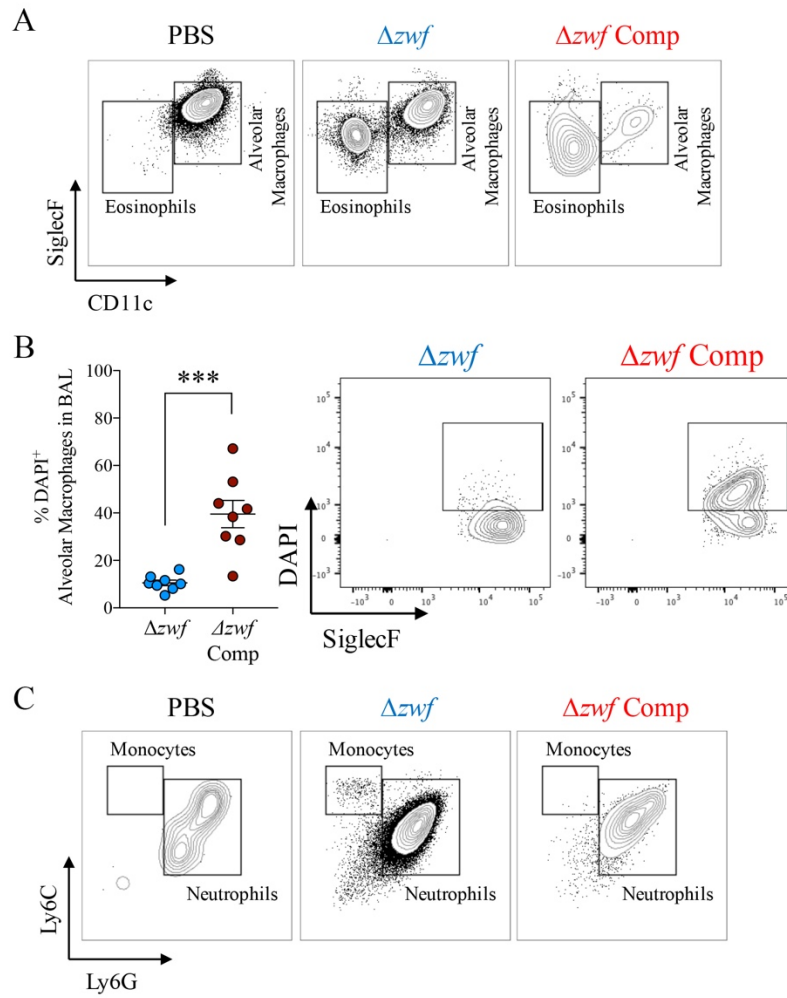


FIGURE S4, related to 5. *P. aeruginosa* G6PDH activity regulates myeloid cells death.

A-C) Representative density plots for live (DAPI⁻) alveolar macrophages (A), DAPI⁺ (dead cells) alveolar macrophages (B) and Ly6C^{high}Ly6G^{low/-} monocytes and Ly6C^{low/neg}Ly6G⁺ neutrophils (C) in BAL of mice uninfected (PBS) or 16h infected with Δzwf and Δzwf complemented PAO1. Data are shown as average +/- SEM. **A-C** are representative from n=2 (7-8 mice total). **B:** t-Student test. ***: $P < 0.001$; ns: non-significant.

FIGURE S5

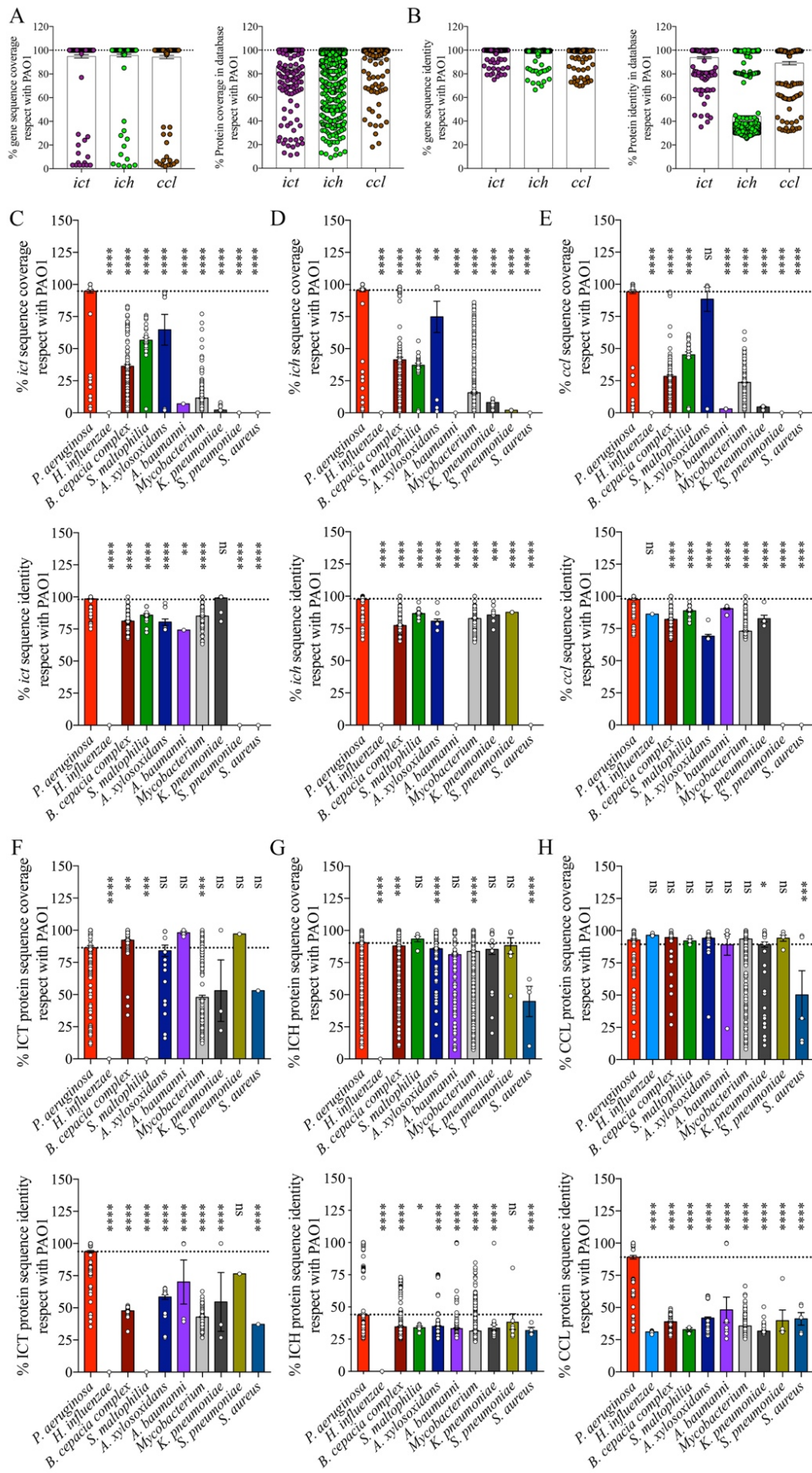


FIGURE S5, related to FIGURE 6. Genes/proteins that regulate itaconate assimilation are conserved in *P. aeruginosa* strains and are found less often in genomes of other respiratory pathogens.

A) *P. aeruginosa* PAO1 *ict*, *ich* and *ccl* genes were compared against all published *P. aeruginosa* genomes (taxid 136841). Upper panel: gene coverage respect with PAO1; lower panel: sequence identity for the coverage matched in the upper panel.

B) *P. aeruginosa* PAO1 ICT, ICH and CCL protein sequences were blasted against all published *P. aeruginosa* genomes (taxid 136841). Upper panel: protein coverage respect with PAO1; lower panel: sequence identity for the protein coverage matched in the upper panel.

C-E) *P. aeruginosa* PAO1 *ict*, *ich* and *ccl* genes were compared against all published genomes for different respiratory pathogens. Upper panel: gene coverage respect to PAO1; lower panel: sequence identity for the coverage matched in the upper panel.

F-H) *P. aeruginosa* PAO1 ICT, ICH and CCL protein sequences were compared against all published genomes for different respiratory pathogens. Upper panel: protein coverage respect to PAO1; lower panel: sequence identity for the protein coverage matched in the upper panel. Blasts were performed at <https://blast.ncbi.nlm.nih.gov/Blast.cgi>. *P. aeruginosa* taxid 136841; *H. influenzae* taxid 727; *B. cepacia* complex taxid 87882; *S. maltophilia* taxid 995085; *A. xyloxydans* 85698; *A. baumannii* taxid 470; *Mycobacterium* taxid 85007; *K. pneumoniae* taxid 573; *S. pneumoniae* taxid 1313; *S. aureus* taxid 1280.

Data are shown as average +/- SEM. Data was analyzed by One-Way ANOVA. *****: $P < 0.0001$; ***: $P < 0.001$; **: $P < 0.01$; *: $P < 0.05$; ns: non-significant.

FIGURE S6

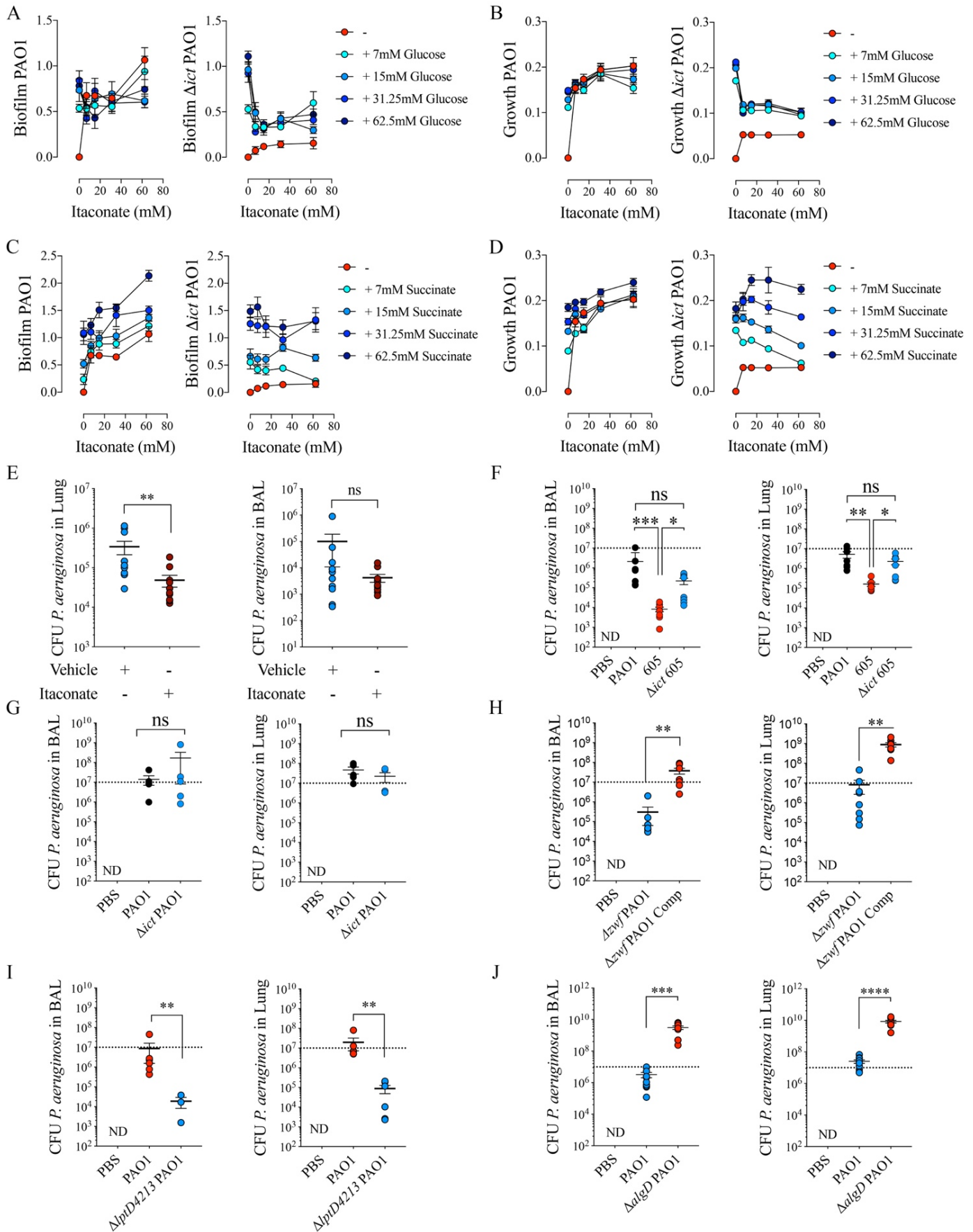


FIGURE S6, related to FIGURE 6. Long-term adaptation to itaconate stress modifies the infective properties of *P. aeruginosa*.

A-D) Itaconate-based biofilm and growth for PAO1 and its isogenic Δict PAO1 mutant cultured overnight in glucose (A-B) or succinate (C-D).

E) CFUs recovered from BAL and lung of WT mice 16h-infected with a collection of 17 CF host-adapted *P. aeruginosa* isolates and treated intranasally with 60mM itaconate. Itaconate treatment was 24h previous CFUs counts.

F-J) CFUs recovered from BAL and lung of mice 16h-infected either with 605 control, Δict 605 or WT PAO1 (F), Δict PAO1 or WT PAO1 (G), Δzwf PAO1 or Δzwf complemented PAO1 (H), $\Delta lptD4213$ PAO1 or WT PAO1 (I) or $\Delta algD$ PAO1 or WT PAO1 (J).

Data are shown as average +/- SEM. All data is from n=2 (in vivo, 5-9 mice in total). **E:** t-Student test; **F-J:** One-Way ANOVA. ****: $P < 0.0001$; ***: $P < 0.001$; **: $P < 0.01$; *: $P < 0.05$; ns: non-significant.

FIGURE S7

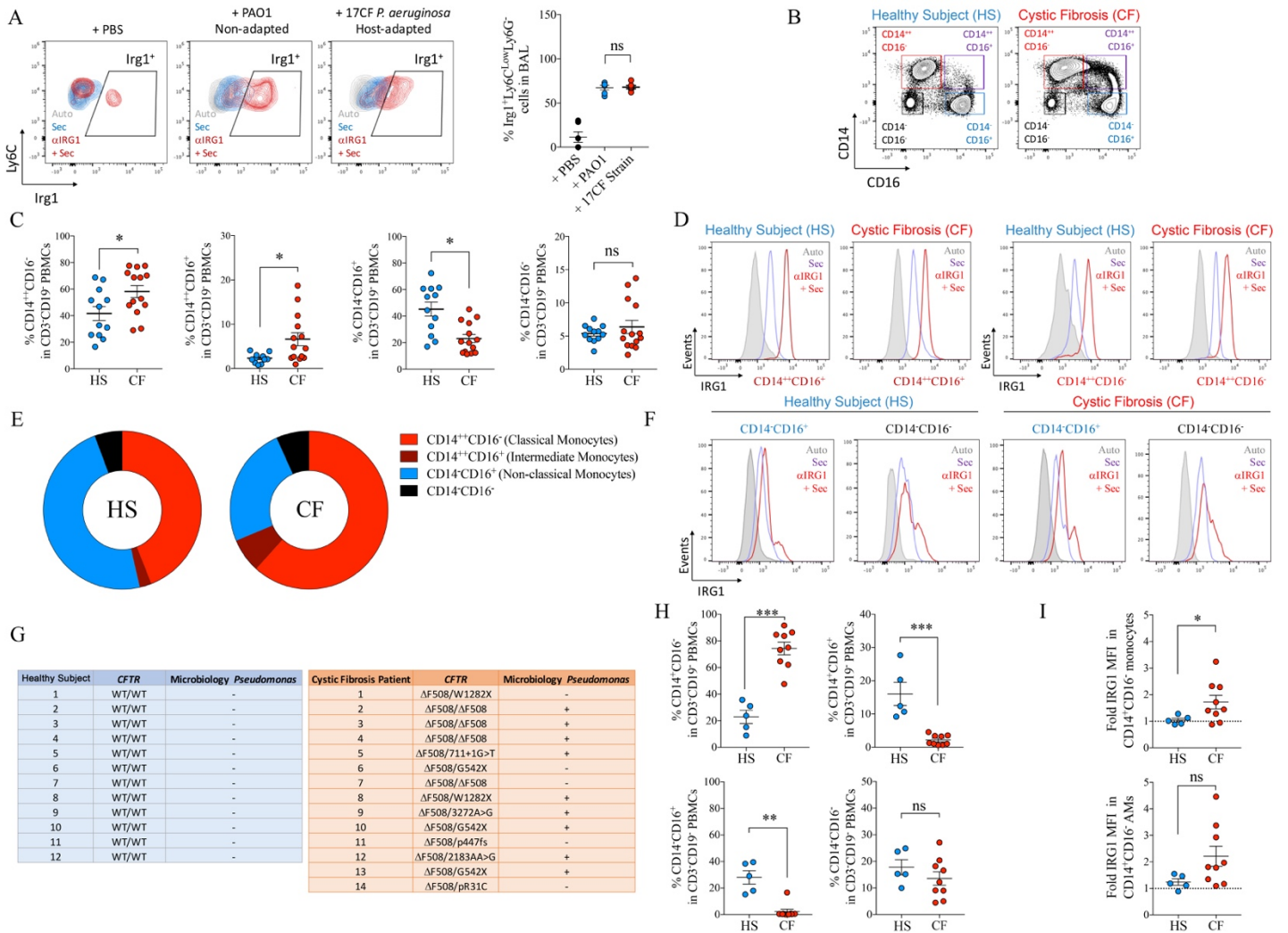


FIGURE S7, related to FIGURE 7. Local and peripheral itaconate-producing cells are associated with *P. aeruginosa* lung infection.

A) Representative density plots (left panel) and percentage of Irg1-expressing Ly6C^{low}Ly6G⁻ monocytes (right graph) from mice treated either with PBS or infected with PAO1 or a collection of 17 CF-host adapted *P. aeruginosa* isolates.

B) Human PBMCs were sorted (DAPI⁻CD45⁺CD3⁻CD19⁻) and analyzed for monocytes using CD14 and CD16 markers by flow cytometry.

C) Dot plots for frequency quantification of the four populations found in B in healthy versus subjects with CF.

D) Intracellular IRG1 levels by flow cytometry in the CD14⁺CD16⁻ and CD14⁺CD16⁺ blood monocyte cells.

E) Frequency quantification of the four populations found in B in healthy subjects versus individuals with CF.

F) Intracellular IRG1 levels by flow cytometry in the CD14⁻CD16⁻ and CD14⁻CD16⁺ blood monocyte cells.

G) List of human samples analyzed depicting *CFTR* mutation involved and whether patients were actively colonized by *P. aeruginosa* (+) or not (-).

H) Percentage of CD14⁺CD16⁻, CD14⁺CD16⁺ (alveolar macrophages), CD14⁻CD16⁻ and CD14⁻CD16⁺ cells in DAPI⁻CD45⁺CD3⁻CD19⁻ sputum cells from healthy subjects and individuals with CF.

I) Fold IRG1 MFI over secondary antibody staining for CD14⁺CD16⁻ and CD14⁺CD16⁺ (alveolar macrophages) sputum cells.

Data are shown as average \pm SEM. A is representative from $n=2$ with a total of 5 mice. Sputum from 9 individuals with CF and 5 healthy subjects were analyzed. In **C**, **H** and **I**, each dot represents a single subject. In **A**, **C**, **H** and **I** data were analyzed by t-Student test. ***: $P < 0.001$; **: $P < 0.01$; *: $P < 0.05$; ns: non-significant.